Astron. Astrophys. 211, 208–216 (1989)

ASTRONOMY AND ASTROPHYSICS

Circumstellar dust around HR 4049: a critical test for theories of interstellar dust★

L.B.F.M. Waters[1], H.J.G.L.M. Lamers[1,2], T.P. Snow[2]★★, E. Mathlener[1], N.R. Trams[1], P.A.M. van Hoof[1], C. Waelkens[3], C.G. Seab[4]★★, and R. Stanga[5]

[1] SRON, Laboratory for Space Research Utrecht, Beneluxlaan 21, 3527 HS Utrecht, The Netherlands
[2] Center for Astrophysics and Space Astronomy, University of Colorado, Campus Box 391, Boulder, CO 80309-0391, USA
[3] Astronomical Institute, Catholic University of Leuven, Celestynenlaan 200 B, B-3030 Heverlee, Belgium
[4] Virginia Institute for Theoretical Astronomy, University of Virginia, Department of Astronomy, P.O. Box 3818, University Station, Charlottesville, VA 22903, USA
[5] European Southern Observatory, Karl Schwarzschildstrasse 2, D-8046 Garching bei München, Federal Republic of Germany

Received November 19, 1987; accepted July 7, 1988

Summary. The properties of the dust around the post-AGB star HR 4049 (B9.5 Ib–II) are derived. There is a large UV deficiency, which is approximately proportional to λ^{-1} but does not show any sign of the 2175 Å absorption feature. The extinction law levels off at longer wavelengths ($\lambda \geq 4500$ Å) producing a circumstellar reddening of $0.19 \leq E(B-V) \leq 0.29$ in the visual. The polarization angle also changes near 4500 Å, suggesting the presence of two grain populations. The IR excess as a function of wavelength ($1 \leq \lambda \leq 100\,\mu$m) can be explained by a simple optically thin dust model with a λ^{-1}-opacity and an r^{-2}-density distribution. The grains responsible for the UV extinction also cause the IR excess. There is evidence for an extended cool (~ 30 K) dust component which is probably a remnant of the AGB wind. The IRAS Low Resolution Spectrum reveals emission features between 7 and 9 μm and at 11.3 μm, while ground based observations show an emission at 3.3 μm, all indicating the presence of polycyclic aromatic hydrocarbons (PAH's). These PAH's do not produce the 2175 Å absorption feature nor the diffuse bands at 5780 and 6614 Å. The consequences for the theories of the 2175 Å absorption feature and the diffuse interstellar bands are discussed.

Key words: stars: HR 4049 – supergiants – circumstellar matter – infrared radiation – dust

1. Introduction

The studies of the properties of interstellar and circumstellar dust suffer from the fact that the lines of sight for which the extinction is studied usually contain a mixture of clouds with different characteristics, thus complicating the interpretation of the observations. Ideally one would like to study the extinction and emission properties in lines of sight which contain a relatively simple mixture of grains in an environment with a known chemical composition and UV radiation density. The line of sight towards the star HR 4049 = HD 89353 may be one of the very rare examples of such a case.

The interstellar extinction towards HR 4049 is small, $E(B-V) < 0.10$, since the star is located at high galactic latitude. Yet the UV extinction is very large and is mainly due to circumstellar grains. These grains do *not* produce an absorption dip at 2175 Å nor diffuse bands at 5780 and 6614 Å. In addition, there is a large IR excess due to circumstellar grains, with a peak near 3.6 μm indicative of dust temperatures on the order of 1200 K. The Infrared Astronomical Satellite (IRAS) low-resolution spectrum shows the presence of two emission features, one from 7 to 9 μm and one at 11.3 μm.

The temperature and the chemical composition of the star which produces this circumstellar material are reasonably well known from photometry and visual spectroscopy. The temperature of the star is about 10,000 K, in agreement with its spectral type of B9.5 I–II. The star is an extremely metal poor Pop II object in transition from the Asymptotic Giant Branch (AGB) phase to the Planetary Nebula phase. The visual spectroscopy indicates that its major photospheric elements are H and C with ratios of C/H $\sim 10^{-3}$ to 10^{-1} and C/O $\sim 10^{+1}$ by number.

These unique properties enable the study of the circumstellar dust, in particular the relation between the 2175 Å feature, the diffuse interstellar bands and the IR emission features for a given chemical composition and temperature.

In Sect. 2 we describe the properties of the star. The UV extinction is discussed in Sect. 3. The IR energy distribution is compared with predictions of an optically thin dust model in Sect. 4. In Sect. 5 we discuss the evidence for an extended cool, $T \simeq 30$ K dust component around the star. The IRAS Low Resolution Spectrum (LRS) is described in Sect. 6. The diffuse band observations are described in Sect. 7. The observed properties of the dust around HR 4049 are compared with theoretical predictions concerning the IR emission features and the 2175 Å absorption feature in Sect. 8.

Send offprint requests to: H.J.G.L.M. Lamers

★ Partly based on IRAS observations. The Infrared Astronomical Satellite was developed and operated by the Netherlands Agency for Aerospace Programs, the U.S. National Aeronautic and Space Administration and the U.K. Science and Engineering Research Council.

★★ Guest Observer of Canada-France-Hawaii Telescope

2. The star HR 4049

The remarkable object HR 4049, classified as B9.5 Ib–II on the basis of its visual spectrum, shows many properties that are unique among hot stars. The energy distribution was discussed by Lamers et al. (1986, hereafter referred to as Paper I). The star has a visual magnitude of $V = 5.50$ and $(B - V) = 0.27$. Assuming an intrinsic color of $(B - V)_0 = -0.02$ for B9.5 supergiants, its extinction is $E(B - V) = 0.29$. Most of this extinction is due to circumstellar material, as will be shown below where it is seen that the interstellar reddening in $E(B - V)$ is <0.10. If the star was a Pop I supergiant with $V_0 \simeq -6$ it would be located about 1 kpc above the galactic plane, which is unlikely for a massive star. Therefore we considered the possibility that HR 4049 is a Pop II star in a post-AGB phase with a low gravity.

The Pop II nature of HR 4049 has recently been confirmed on the basis of a study of the optical spectrum (Lamers et al., in preparation, hereafter called Paper II). The optical spectrum shows 28 Balmer absorption lines, confirming the low gravity in the atmosphere. No other lines are conspicuous in the visual spectrum except those of neutral carbon and neutral oxygen. From a simple curve of growth analysis an abundance ratio of C/H $\sim 10^{-3}$ to 10^{-1} and O/C $\sim 10^{-1}$ was found. Lambert et al. (1988) determined the carbon and oxygen abundances for HR 4049 from visual and near-IR spectroscopy. Although these authors use rather low effective temperatures between 6400 K and 8500 K, the C/O ratio they determined does not depend strongly on $T_{\rm eff}$. They find $[{\rm C/O}] \approx 0.6$, so C is a factor 4 overabundant relative to oxygen in the Sun. In Paper II it is shown that the low resolution IUE spectrum is dominated by C II lines, indicating a high carbon abundance. This agrees qualitatively well with the assumption that the star is in a post-AGB phase. Since no metal lines were detected in the visual spectrum, the metallicity must be very low.

A comparison between $T_{\rm eff} = 10{,}000$ K and $\log g = 2.0$ of the star, derived from the Balmer lines, and the predicted evolutionary tracks of post-AGB stars by Schönberner (1983) indicates a mass of 0.54 $M_\odot$, a radius of 12 $R_\odot$, a luminosity of 1.3 $10^3 L_\odot$ and a distance of about 400 pc (Paper II). The star is a long-term photometric variable with a characteristic timescale of about 430 days and a visual amplitude of 0.4 m. The amplitude of the variability decreases towards longer wavelengths, and is almost zero for $\lambda \gtrsim 2.2\,\mu$m (Waelkens et al., in preparation).

The line profiles in the visual spectrum show clear evidence for outflow: all absorption lines are blue shifted by about -20 to $-60\,{\rm km\,s^{-1}}$. The higher Balmer lines (H20 to H30) have a larger outflow velocity than Hα to Hγ, indicating that the wind is decelerated, after an initial acceleration. The smallest velocities are found in the C I lines, which are formed the farthest outward. A very rough estimate of the mass loss rate, based on the Hα emission component, suggests a value on the order of $10^{-7}\,M_\odot\,{\rm yr}^{-1}$. With such a high mass loss rate the density of the wind at about 10 R_* would be on the order of 10^9 atoms cm^{-3}.

3. The circumstellar extinction

The energy distribution of HR 4049 in the UV was measured by the ANS ultraviolet telescope and the S2/68 experiment. The observed energy distribution, which was presented in Paper I, showed a strong UV deficiency without any sign of an absorption dip near 2175 Å. In Paper II we have compared the energy distribution with the intrinsic distribution of four supergiants with about the same spectral type. The result is shown in Fig. 1 in terms of a logarithmic flux deficiency due to circumstellar dust versus λ^{-1}. Three cases are presented with the flux distribution of HR 4049 corrected for interstellar extinction with $E(B - V)_{\rm IS} = 0$, 0.1 and 0.2. The figure shows that in all cases the circumstellar extinction varies approximately as λ^{-1} from $1/\lambda = 2$ to $6.5\,\mu{\rm m}^{-1}$. The figure also shows that an adopted interstellar reddening of $E(B - V)_{\rm IS} > 0.1$ produces an artificial bump in the energy distribution at 2175 Å, $1/\lambda = 4.6\,\mu{\rm m}^{-1}$. Therefore the interstellar contribution to $E(B - V)$ is probably less than about 0.1 mag. This is in agreement with the small distance of the star and with the very weak diffuse interstellar bands (Sect. 7). Since the total extinction is $E(B - V)_{\rm tot} = 0.29$, the remaining part of this extinction must be due to the circumstellar material, with $0.19 < E(B - V)_{\rm cs} < 0.29$.

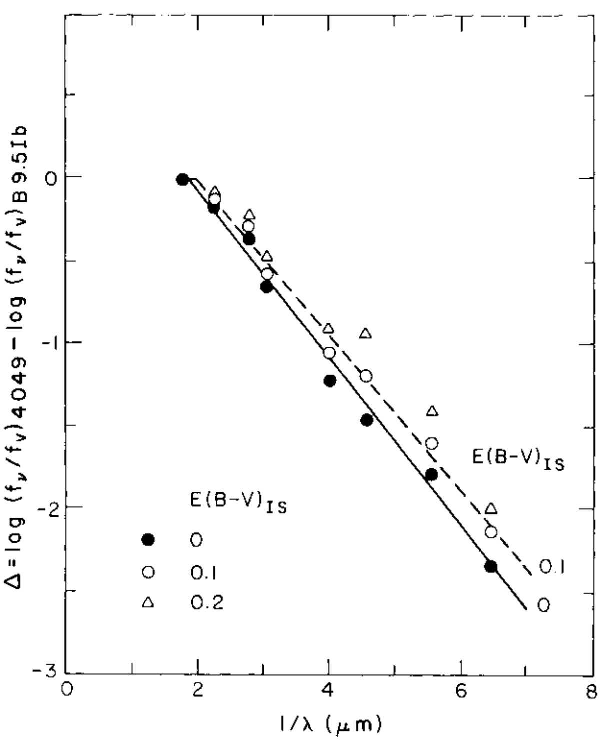

Fig. 1. The logarithmic UV deficiency of HR 4049 compared to a normal B9.5 Ib star and normalized to the V-band is plotted versus $1/\lambda$. The symbols are the observed deficiencies for three values of the adopted $E(B - V)_{\rm IS}$. The straight lines are the best fits described by Eq. (1a) (solid line) for $E(B - V)_{\rm IS} = 0$ and Eq. (1b) (dashed line) for $E(B - V)_{\rm IS} = 0.10$

The data plotted in Fig. 1 show that the circumstellar extinction varies as

$$\Delta \simeq -0.51\{\lambda^{-1} - 1.89\} \quad \text{if } E(B - V)_{\rm IS} = 0.0 \tag{1a}$$

$$\Delta \simeq -0.47\{\lambda^{-1} - 1.98\} \quad \text{if } E(B - V)_{\rm IS} = 0.1 \tag{1b}$$

where Δ is the logarithm of the flux deficiency, which has to be multiplied by -2.5 to find the deficiency in magnitudes. The data point at $1/\lambda = 2.8$ (U-band) is above these relations. This may be due to the variability of the star (see Sect. 2), since the ANS measurements were not obtained simultaneously with the UBV photometry.

The λ^{-1} extinction law extends to at least 1550 Å ($\lambda^{-1} = 6.5\,\mu^{-1}$) which is the shortest wavelength measured by ANS.

The extinction laws of Eqs. (1a) and (1b) predict a circumstellar extinction of $E(B-V)=0.48$ and 0.34 mag. respectively, which is higher than the total extinction of $E(B-V)=0.29$. This difference may be due to variability, or to deviations from the linear extinction law in the visual.

Although our data show little differential extinctions in the visible part of the spectrum, recent polarization data (Joshi et. al., 1987) indicate that there may be significant gray extinction. Visible and infrared polarimetry show that HR 4049 emits polarized light probably due to scattering by circumstellar dust that has a slightly nonspherical distribution around the star. The small wavelength dependence of the polarization along with the low differential extinction (i.e. low reddening) indicates that the grains responsible for the polarization must be large (Joshi et al. suggest 0.8 μm as the typical size of these grains.)

The polarization results also show another interesting phenomenon for HR 4049. The polarization changes rapidly with wavelength near 4500 Å, where the extinction curve levels off. This is interpreted as due to a second population of smaller ($\sim 0.05\,\mu$m) grains having a different nonspherical distribution around the star, which dominate the polarization at short wavelengths. Thus, the polarization data suggest that HR 4049 has two distinct dust shells, one consisting of rather small grains, and the other consisting of large grains.

4. The IR excess

4.1. The determination of the IR excess

The IR energy distribution was measured from *UBVRIJHKLM* and IRAS photometry at 12, 25 and 60 μm (Paper II). In order to determine the IR excess we used a model atmosphere of Kurucz (1979) with $T_{\rm eff}=10{,}000$ K and $\log g=1.5$ to estimate the photospheric flux in the IR. The model fluxes and the observations are normalized to the flux in the V-band. The exact value of the IR excess depends somewhat on the adopted value of the interstellar extinction. Since this value is uncertain (see Sect. 3) we used two values of $E(B-V)_{\rm IS}=0.10$ and 0.20 to calculate the IR excess and to show the effect of the uncertainty in $E(B-V)$. The IRAS observations and the visual and near-IR photometry were not taken simultaneously. However, extensive monitoring of the photometric variability has shown (Paper II) that the amplitude of the variability decreases towards the IR. No evidence for variability $> 0^{\rm m}.1$ is found for $\lambda > 2.2\,\mu$m. Therefore we can combine the IRAS and groundbased IR observations. The resulting excess fluxes are listed in Table 1. The differences between the excess fluxes for $E(B-V)=0.1$ and 0.2 are significant for $\lambda < 2.2\,\mu$m, and we adopted the average of both values (Table 1).

4.2. An optically thin dust model

The IR excess can be explained by optically thick dust with a blackbody temperature of 1250 K. However, the excess flux energy distribution can equally well be fitted by small optically thin dust grains that do not radiate as blackbodies.

We use the optically thin dust model described by Sopka et al. (1985) to fit the observed IR excess energy distribution. Although this model probably is not correct for HR 4049, because of the UV deficiency, it gives a first order approximation of the properties of the dust shell. The parameters derived from the fit are strongly dependent on the unknown properties of the dust grains.

Table 1. The IR excess of HR 4049

λ (μm)	Log f[a] $E(B-V)=0.1$	Log f[a] $E(B-V)=0.2$	Log f[a] adopted
1.25	−21.978	−22.101	−22.035 ± 0.05[b]
1.65	−21.771	−21.820	−21.795 ± 0.02
2.20	−21.452	−21.459	−21.455
3.60	−21.117	−21.114	−21.115
4.80	−21.140	−21.136	−21.138
12.00	−21.462	−21.463	−21.462 ± 0.04
25.00	−22.141	−22.143	−21.142 ± 0.04
60.00	−22.879	−22.880	−22.880 ± 0.06

[a] The fluxes are given in units of erg cm^{-2} s^{-1} Hz^{-1}.
[b] The error estimate is based on the difference between the excess fluxes using $E(B-V)=0.1$ and 0.2 for $\lambda=1.25$ and 1.65 μm, and on the photometric errors for $\lambda=12$, 25 and 60 μm. The error estimate does not include the errors due to variability.

The dust grains radiate with an emission efficiency $Q(\nu) \sim \nu^p$ It is assumed that the dust grains are in thermal equilibrium with the stellar UV radiation field. The resulting temperature distribution of the dust grains under this assumption is

$$T(r) = T_0 (r/R_*)^{-2/(4+p)} \tag{2}$$

where T_0 is a normalization temperature. Equation (2) is correct for a dust shell which is optically thin at all wavelengths. The UV energy distribution of HR 4049 clearly indicates that the dust is optically thick in the (far)-UV. In that case one would expect an exponential decrease of the dust temperature with radius. However, in view of the unknown properties of the dust grains and the effect these properties have on the temperature structure, we use Eq. (2). The number density distribution of the dust grains is given by:

$$n_d(r) = n_0 (r/R_*)^{-m}. \tag{3}$$

The dust is assumed to be distributed spherically symmetric around the star from inner radius r_0 to outer radius r_1. Furthermore, we assume that the grain size is constant, which is probably not correct (Sect. 5). The effect of a size distribution of the dust grains on the resulting infrared energy distribution was considered by Mezger et al. (1982) and more recently by Wolfire and Cassinelli (1986). The thermal equilibrium temperature of dust grains depends on the size of the grains, the smaller grains being hotter. Mezger et al. (1982) show that in the case of a grain size distribution the IR spectrum is well represented by that of an isothermal cloud of dust grains with one average size. We expect that the effect of the density distribution on the temperature distribution of the dust grains is much more important than that of a size distribution.

For very small ($a < 50$ Å) particles the concept of thermal equilibrium breaks down. These grains are temporarily heated to high (about 1000 K) temperatures due to the absorption of energetic UV photons (e.g. Sellgren, 1984). As we will show in Sect. 5, evidence for the presence of such small grains is found in the IRAS Low Resolution Spectrum. The contribution of these particles to the IR flux is not taken into account in our model because calculations of Puget et al. (1985) indicate that the contribution of these small particles to the continuum is negligible compared to the IR flux due to the larger grains that are in thermal equilibrium with the star.

4.3. Results of the fitting

We fitted a range of models to the observed excess flux energy distribution (Table 1). Unfortunately, the relatively large number of model parameters does not allow the determination of a unique solution. However, the possible range of some of the model parameters can be restricted. It is reasonable to assume that the number density distribution of the dust grains (Eq. (3)) follows an inverse square law, i.e. a constant velocity outflow is assumed. There is evidence that the velocity structure of the wind of HR 4049 is rather complex, showing a deceleration after an initial acceleration (Sect. 2). However, this deceleration occurs relatively close to the star (Paper II) and the region where the dust is formed is situated further outward, so the approximation of $\rho \sim r^{-2}$ is reasonable.

The shape of the UV energy distribution can be used to estimate the value of p. In Sect. 3 it is shown that the dust particles have an absorption efficiency proportional to λ^{-1}. Therefore, we can adopt $p = 1$ for the particles which are responsible for the IR excess. This is only valid if the dust particles responsible for the UV extinction also produce the IR excess, which is strongly supported by the fact that the amount of energy absorbed in the UV is roughly the same as the amount of energy radiated in the IR (Paper I).

The normalization temperature T_0 can be found from the method given by Sopka et al. (1985), yielding:

$$T_0 = T(r = R_*) = 4.802\,10^{-11} \times \left[5.397\,10^{45}\{(p+3)!\}^{-1} \int_0^\infty F_\nu^* \nu^p \, d\nu\right]^{1/(4+p)} \qquad (4)$$

The integral in Eq. (4) was evaluated using the Kurucz (1979) model with $T_{\rm eff} = 10^4$ K and $\log g = 1.5$ (Paper I), yielding T_0 7800 K. We calculated a number of dust models with $p = 1, m = 2$ and various values of r_0 and r_1, the inner and outer radius of the dust shell. We found a "best fit" for $r_0 = 90R_*$ and $r_1 = 4450R_*$, and the fit is shown in Fig. 2 (solid line). This figure shows that the observed excess flux energy distribution can be explained by the simple optically thin dust model. The 1.25 μm flux is somewhat higher than predicted by our model, however, this flux may be affected by variability of the star (Sect. 4.1).

We stress that the model parameters derived above provide no unique solution. For instance, a satisfactory fit to the observed energy distribution can also be found for a model with $T_0 \simeq$ 8350 K, $p = 2$, $r_0 = 440R_*$ and $r_1 = 4\,10^7\,R_*$. This fit is shown as the dotted line in Fig. 2.

5. The extended 100 μm emission

We searched for the presence of an additional cool dust component with temperatures of the order of 30 K by plotting the IRAS detector response of the 100 μm data as a function of time. There is some evidence for 100 μm flux at the position of HR 4049, although the flux level is low. In order to improve the signal to noise ratio, we used a one-dimensional co-add routine developed at the SRON Space Research Laboratory at Groningen by

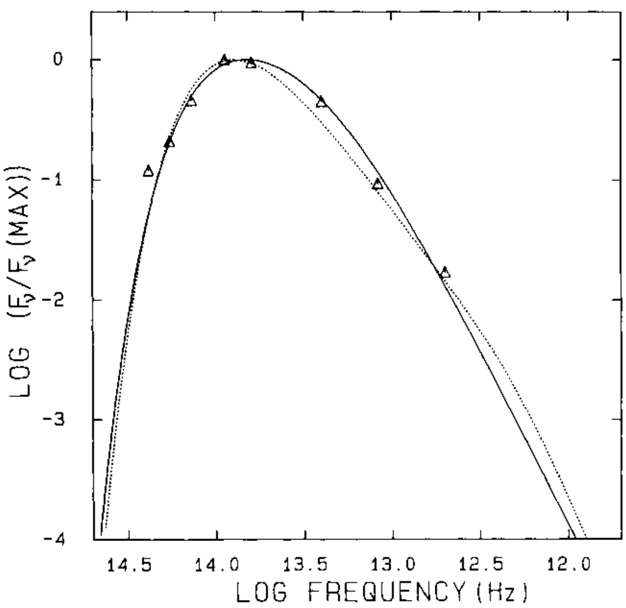

Fig. 2. The excess flux energy distribution of HR 4049 is plotted versus log frequency. The flux is normalized to the maximum flux (Table 1). The solid line is the resulting energy distribution of an optically thin dust model with parameters $p = 1$, $m = 2$ (Eq. (2)), $T_0 = 6200$ K (Eq. (4)) and $r_0 = 50R_*$ and $r_1 = 2500R_*$. The dotted line is the same, but with parameters $T_0 = 6900$ K, $p = 2$, $r_0 = 250R_*$ and $r_1 = 2\,10^7\,R_*$

J. Wollaert. This routine uses the observed peak position of the source at 12 and 25 μm to align the detector responses at 60 and 100 μm. In Fig. 3, the resulting coadded detection of HR 4049 in the 4 IRAS bands is shown.

Figure 3 clearly shows that HR 4049 is a point source at 12 and 25 μm. The width of the peak is due to the width of the detectors at 12 and 25 μm. At 100 μm the peak clearly is wider than expected for a point source. The maximum of the peak is only $-0.012^\circ = 0'.75$ from the expected position. Since this is at the limit of the accuracy of the position determination at 100 μm, we conclude that the maximum is due to HR 4049. There is an additional 100 μm source at $-0^\circ.075 = 4'.5$ from HR 4049 which produces a second maximum on the left side of the maximum emission peak. This second peak is *not* due to HR 4049 as it was absent in some of the slightly shifted scans, when that source did not pass the detector. This second source must be cool because it is invisible at 12 and 25 μm.

In order to study this 100 μm emission in more detail a two-dimensional co-add of the IRAS 100 μm scans was made using the GEISHA data processing system developed in Groningen, The Netherlands. The resulting map of HR 4049 at 100 μm is shown in Fig. 4, along with a map of the point source o Ceti (Mira). Indicated in Fig. 4 are the contours for 0.5 times the peak height and 0.25 times the peak height. It is clear from Fig. 4 that the 100 μm emission of HR 4049 is extended over about 15'. Assuming a distance of 400 pc (Sect. 2), the linear diameter of the emitting region is 1.8 pc. Since the extended emission is not present at 12, 25 and 60 μm, the temperature of the dust responsible for it must be ≤ 30 K.

This extended cool component cannot be due to the same dust which produces the large excess observed between 2 and 25 μm for two reasons. First of all the extrapolation of the dust model fits shown in Fig. 2 predict a flux level at 100 μm on the

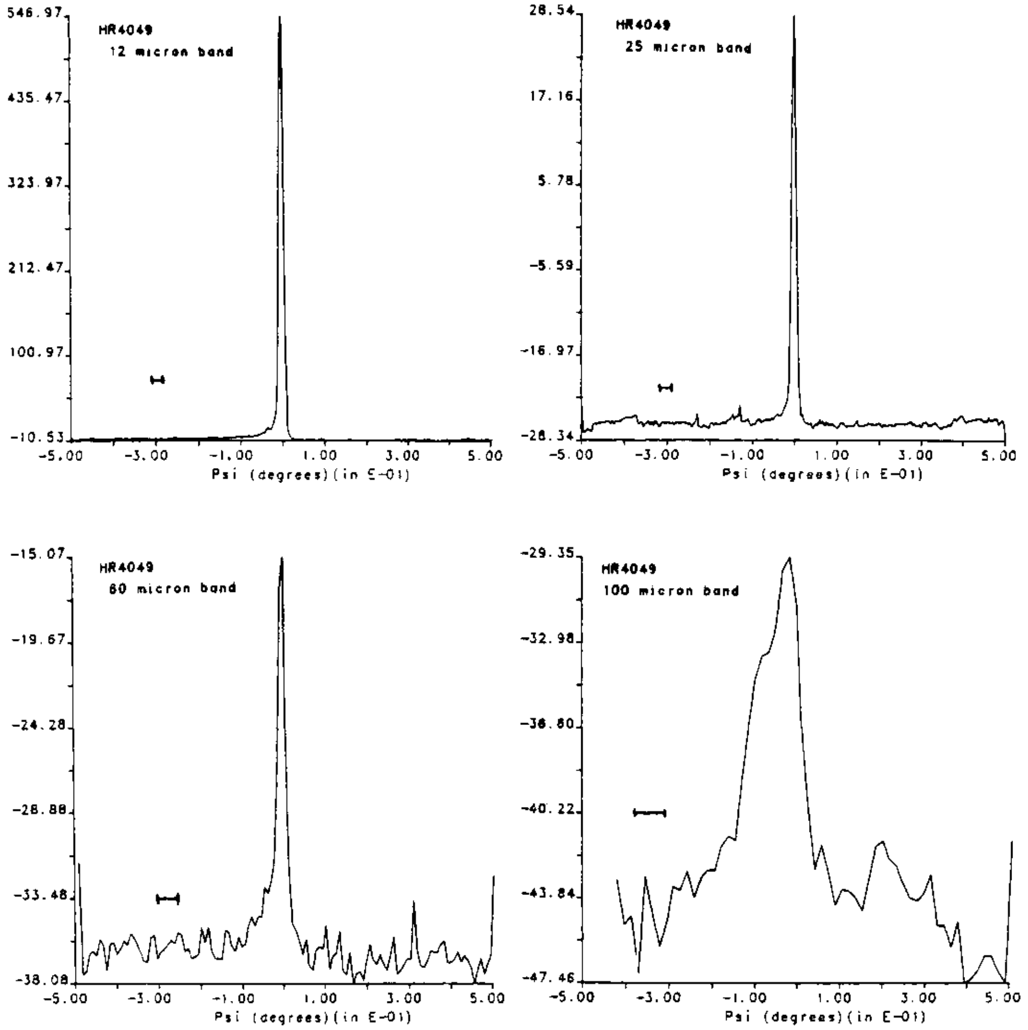

Fig. 3. The co-added one-dimensional detector responses as a function of position on the sky for HR 4049 at 12, 25 60 and 100 μm are shown. In each panel the width of a point source near the continuum, (i.e. at the base of the peak) is indicated. HR 4049 is a point source at 12 and 25 μm and is clearly extended at 100 μm with a width of the peak at the base of about 15′

order of 0.2 Jy, whereas the observed flux at 100 μm is about 1 to 2 Jy. Secondly, the dust model with $p = 1$ and $T_0 = 7800$ K predicts that a temperature of 30 K is reached at a distance of $1.1\,10^6\,R_* = 0.3$ pc whereas the observed radius of the source is about 0.9 pc.

This extended cool dust emission may be due to material ejected by the star when it was still in the AGB phase. Assuming a typical ejection velocity of 20 km s^{-1}, the dust must have been ejected about $5\,10^4$ yr ago. This is a typical timescale for evolution from the AGB to a hot phase. Schönberner (1983) has shown that the time required by a star of 0.546 $M_\odot$ to reach $T_{\rm eff} = 10^4$ K after leaving the AGB is about $3\,10^4$ yr. So, considering the uncertainties in the estimated size of the extended emission, in the velocity and in the predicted post-AGB evolutionary timescales, it is likely that the extended cool component is the remnant of the AGB ejection.

6. The infrared spectrum

Two IRAS Low Resolution Spectra of HR 4049 were taken during the mission in 1983. For a description of the LRS instrument and its operation we refer to the IRAS Explanatory Supplement (1985). We use the average of the two spectra as published in the IRAS Atlas of low-resolution spectra (1986). The spectrum is plotted in Fig. 5. The spectrum is rather smooth, and noisy for $\lambda > 16\,\mu$m. The spectrum is classified in category "80" which means that an 11.3 μm emission feature is present without other atomic lines. This is typical for H II regions and emission line stars. The feature at 11.3 μm is clearly visible in Fig. 5. In order to search for other features in the LRS spectrum, we fitted a powerlaw to the continuum between 9 and 12 μm, excluding the 11.3 μm feature. The fit is shown in Fig. 5 as the dotted line. The difference between the observed spectrum and the dotted line is plotted in Fig. 6. Apart from the 11.3 μm feature, an excess relative to the estimated continuum is seen between about 7 and 9 μm. This feature and the 11.3 μm feature are also observed in planetary nebulae (Pottasch, 1984) and in reflection nebulae around hot stars (Sellgren, 1984).

Sakata et al. (1984) suggested that the 11.3 μm feature is due to quenched carbonaceous composite (QCC). Sakata et al. (1987) show that the IR spectrum of so called oxydised QCC shows the 7.7 and 8.6 μm emission features. However, the relative strength of the features does not correspond to the observations and a very strong feature is found at 6.9 μm, which is not observed in spectra of objects showing the other features. Furthermore, Sakata et al. (1983) show that QCC absorbs strongly at 2175 Å which would give rise to a 2175 Å extinction bump. Clearly this

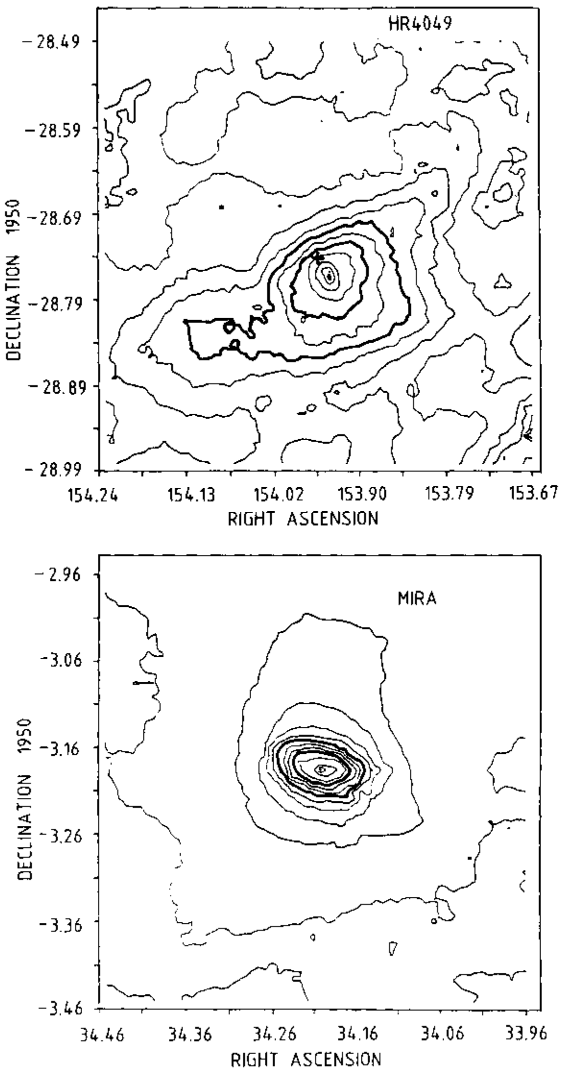

Fig. 4. The two dimensional co-add of HR 4049 (top panel) and Mira (bottom panel), calculated using the GEISHA system. Indicated are contours of constant flux level. The contours at 0.5 times the peak flux and 0.25 times the peak flux are bolded. HR 4049 clearly is more extended at 100 μm than Mira, which is a point source

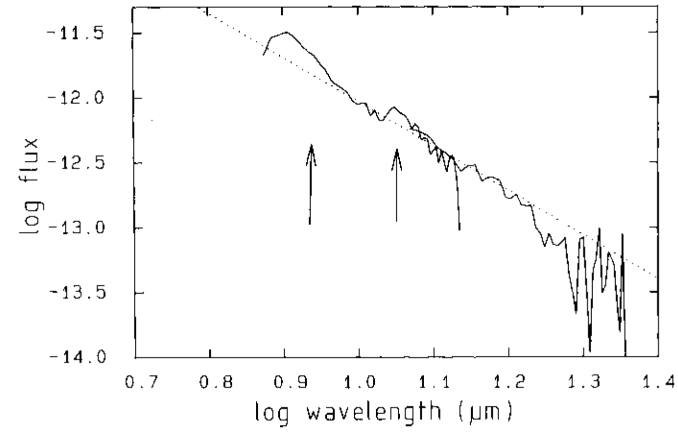

Fig. 5. The IRAS Low Resolution Spectrum is plotted versus log wavelength. The dotted line represents the estimated continuum. Notice the excess relative to the dotted line between 7 and 9 μm and around 11.3 μm

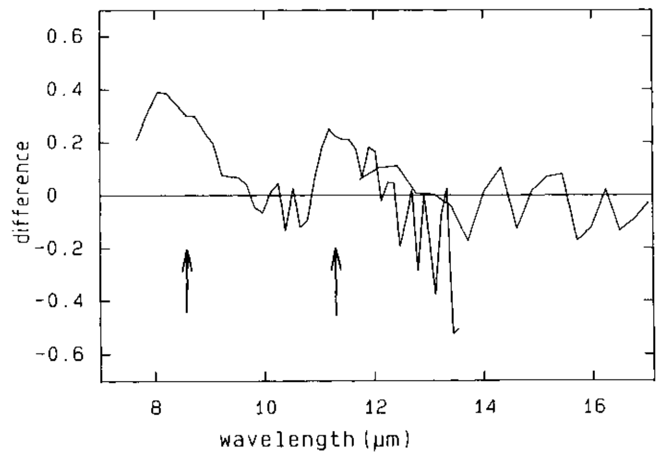

Fig. 6. The difference between the observed spectrum and the dotted line (shown in Fig. 5), i.e. $((F_{\rm obs} - F_{\rm cont})/F_{\rm cont})$ is plotted versus wavelength. The emission features at 7–9 μm and 11.3 μm are clearly visible, indicating the presence of Polycyclic Aromatic Hydrocarbons

absorption is absent in HR 4049 so we can exclude QCC as dust grains in HR 4049. Léger and Puget (1984) show that the 7.7, 8.6, and 11.3 μm emission features could be due to polycyclic aromatic hydrocarbons (PAH). They found a good match between the laboratory spectrum of a PAH and the observed spectrum of the planetary nebula NGC 7027. We conclude that PAH's may be present in the dust around HR 4049.

Another possible carrier of the IR emission bands is hydrogenated amorphous carbon (HAC) (Borghesi et al., 1987). However, Borghesi et al. show that the 3.3 μm emission feature should be absent in dust with temperatures as high as are observed in HR 4049 (higher than 400 K). Furthermore, some emission features, which are present in the laboratory spectra of HAC, are not observed in HR 4049. We therefore assume that the IR emission features in HR 4049 are due to PAH's.

The spectrum of HR 4049 around 3.3 μm (Fig. 7) was obtained by one of us (R.S.) on March 23, 1986 with the 1 m telescope at ESO, using an InSb detector with a circular variable filter resulting in a resolution of $\lambda/\Delta\lambda \simeq 80$. The standard IR techniques of chopping the signal and beam switching the telescope were adopted. The spectrum was calibrated adopting the star HR 4802 as a standard.

The emission line of 3.28 μm is one of the most prominent lines in reflection nebulae and planetary nebulae and is among the features usually attributed to PAH's (Léger and Puget, 1984). Thus the case for circumstellar PAH's in HR 4049 is very strong.

7. The diffuse bands

The recent interest in PAH's as the possible source of the unidentified infrared emission features has led to suggestions that PAH's might be responsible for other phenomena. One such suggestion (Crawford, et al., 1985) is that ionized PAH's might be the carriers of the unidentified diffuse interstellar bands (DIB's). Laboratory data show that ionized PAH's have absorption bands in the visible, and abundance arguments indicate that they are sufficiently

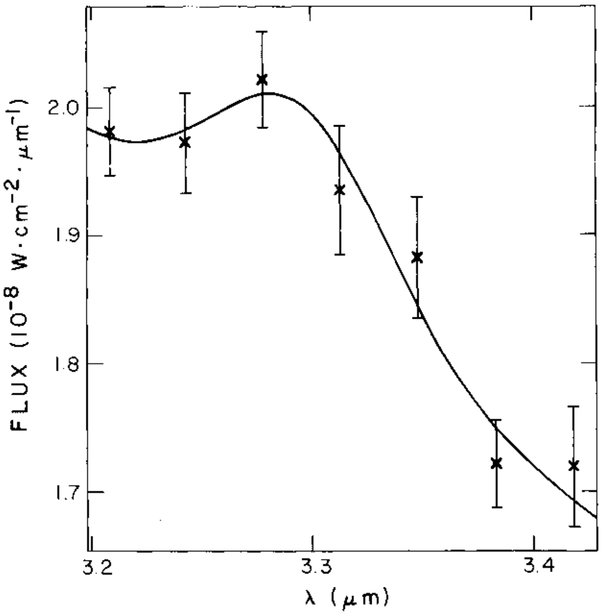

Fig. 7. The near-IR spectrum of HR 4049 near 3.3 μm. This observation, although noisy, suggest the presence of an emission feature near 3.28 μm which is probably due to PAH's. The full line is a least square fit through the data, consisting of a linear continuum and a gaussian emission (see text)

common in the interstellar medium. Unfortunately, it is very difficult to design laboratory experiments to directly measure the spectra of ionized PAH's, so there as yet is no confirmation of the hypothesis that they are responsible for the DIB's.

The circumstellar dust around HR 4049 might provide a very significant test of the hypothesis, however. If the 11.3-micron feature is indeed due to PAH's, then a search for DIB's in the circumstellar material will test whether PAH's form DIB's. Therefore, when two of us (T.P.S. and C.G.S.) had observing time recently for another DIB project, we took advantage of the opportunity to observe HR 4049.

The observations were made on the 3.6-m Canada-France Hawaii Telescope on 6 February, 1987. The coudé spectrograph was used with a Reticon detector consisting of a linear array of 1872 diodes. Each diode corresponded to 0.072 Å, so the effective resolution was 0.144 Å and the coverage was 138 Å. The quantum efficiency of the detector in the red is close to 60%, so we achieved high-quality data on HR 4049. We observed the DIB wavelengths at 5780.41 Å and 6613.63 Å (Herbig, 1975) with S/N ratios of 190 and 160, respectively.

Figure 8 shows the spectra. At 6614 Å no feature was seen, with an equivalent width upper limit of 4.2 mÅ. At 5780 Å there is a broad shallow absorption feature, but its position is clearly separated from the expected position (indicated by an arrow) by 1.0 Å which corresponds to 52 km s^{-1} if the band were in the rest frame of the star. The radial velocity of the star, listed in the Bright Star Catalogue is -33 km s^{-1}, but it might be as small as -17 km s^{-1} (Paper II). We therefore attribute the observed feature to DIB absorption arising in foreground material. Its equivalent width of 49 mÅ corresponds to an interstellar colour excess of $E(B-V)$ 0.05 to 0.10 (see correlations published by Josafatsson and Snow, 1987; by Krelowski and Walker, 1987; or by Federman et al., 1981). We can in fact use the normal correlation between the 5780 Å strength and reddening to place a rough limit on the amount of foreground reddening toward HR 4049; we argue that this limits the foreground reddening to $E(B-V) < 0.10$, consistent with our estimates based on the strength of the 2175 Å feature (Sect. 3).

The absence of circumstellar DIB absorption toward HR 4049 may be interpreted as casting strong doubts on the hypothesis that the DIB's are due to ionized PAH's. We caution that it has not yet been proven that the 11.3-micron feature is due to PAH's, and we point out that even if it is, the 11.3-micron emission could be coming from material not directly in the line of sight to the star. If the infrared feature arises in an extended disk or shell, for example, then our line of sight for absorption measures against the star might not intersect a sufficient column density of PAH's to produce detectable absorption. It is worth noting, however, that our modeling of the infrared excess implies a hydrogen column density through the circumstellar shell of roughly 10^{21} cm^{-2}, easily sufficient to produce observable DIB's in ordinary inter-

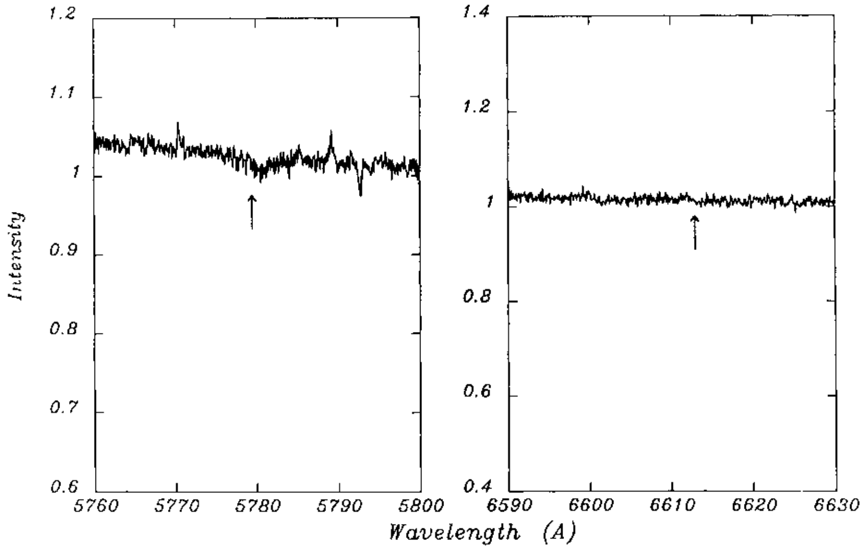

Fig. 8. The diffuse band data. This shows the CFHT spectra of the regions around the diffuse features at 5780 and 6613A. Arrows indicate the expected band positions, if they were in the rest frame of the star. No feature is seen at 6613Å, and the apparent 5780Å band is shifted by about +55 km^{-1} with respect to the rest frame of the star. We attribute this feature to foreground reddening

stellar material. Thus, our result may be taken as evidence against PAH's as the carriers of the DIB's.

8. Summary of the observations of circumstellar matter around HR 4049

We briefly summarize the information about the star HR 4049 and its surrounding matter.

1. HR 4049 is a metal poor post-AGB star, which is extremely carbon-rich: $C/H \sim 10^{-3}$ to 10^{-1}, $O/C \sim 10^{-1}$. The star has a strong stellar wind with $\dot{M} \sim 10^{-7} M_{\odot}\,\mathrm{yr}^{-1}$ and a velocity of the order of 20 to $60\,\mathrm{km\,s^{-1}}$.
2. The distance is 400 pc and the interstellar extinction is small: $E(B-V) < 0.10$ (Sects. 3 and 7).
3. There is a strong UV deficiency which varies as λ^{-1}, starting at about 5000 Å and reaching 5.5 ± 0.3 mag at 1550 Å.
4. There is no sign of the 2175 Å absorption, with an upper limit of $E(B-V) = 0.1$ if we assume the standard interstellar extinction curve.
5. The circumstellar matter around HR 4049 does not produce diffuse band absorption at 5780 and 6614 Å. The weak feature near 5780 is of interstellar origin.
6. Polarization measurements indicate that HR 4049 has a population of large ($\sim 0.8\,\mu$m) grains in addition to the small ones responsible for the UV deficiency. These large grains must produce some gray extinction, and probably form a distinct dust shell, separate from the one formed by the small grains.
7. The IR excess resembles a black-body curve with $T = 1250$ K and an effective area of $800\pi R_*^2$. However, it can be matched also by optically thin dust with a density distribution of $n \sim r^{-2}$ within a region of $90 \lesssim r \lesssim 4500 R_*$.
8. The amount of energy absorbed in the UV by circumstellar dust is about 20% less than the energy emitted in the IR excess. (Paper I), indicating that the IR excess is due to a reradiation of the absorbed UV flux and the absorbed visible flux due to the large grains inferred from the polarization data.
9. There is an extended $100\,\mu$m emission feature with $T \sim 30$ K and a diameter of about 1.8 pc, which is probably the remnant of the AGB wind.
10. The IRAS LRS spectrum shows the presence of the $11.3\,\mu$m emission feature and an emission between 7 and $9\,\mu$m.

9. Discussion

In this paper, we studied the properties of the circumstellar dust around HR 4049. We show that the dust particles responsible for the UV extinction are also responsible for the IR excess emission. We use a simple optically thin dust model to interpret the IR excess as a function of wavelength, in which the density distribution of the dust particles follows an inverse square law (i.e. appropriate for constant velocity outflow), and with an emission efficiency of the dust particles $Q(\nu) \sim \nu^p$ with $p = 1$. The IR excess can be fitted by such a circumstellar dust cloud which extends from about $90 R_*$ ($8\,10^{13}$ cm) to $4\,10^3\,R_*$ ($4\,10^{15}$ cm).

HR 4049 does not seem to show any of the red continuum emission that is observed in objects like the Red Rectangle (Cohen et al., 1975) and reflection nebulae (Witt and Schild, 1985; Sitko et al., 1981). This could indicate that its carrier is destroyed in the presence of high radiation density.

The IRAS Low Resolution Spectrum shows the presence of emission features at about 8.6 and at $11.3\,\mu$m, suggesting that polycyclic aromatic hydrocarbon grains (PAH's) constitute part of the dust around HR 4049. Apparently these PAH's survive the strong UV radiation field of HR 4049.

It is interesting to speculate about the origin of the PAH's in HR 4049. The fact that PAH's are usually detected in the vicinity of strong UV sources such as the central stars of planetary nebulae or H II regions near hot stars (Dwek et al., 1980) suggest that they are the result of destruction of larger grains. The UV deficiency of HR 4049 indicates the presence of circumstellar grains of sizes up to about 300 Å, formed in the outflowing wind. The PAH's around HR 4049 may be a result of the destruction of these grains, perhaps in shocks where the present higher velocity wind collides with remnant material from earlier mass loss phases.

In view of the chemical composition of the atmosphere of HR 4049 it is not surprising that the dust grains in HR 4049 are composed of carbon and hydrogen. The spectroscopic study (Paper II) shows that HR 4049 is very metal poor and has a very high C/H ratio on the order of 10^{-3} to 10^{-1}.

We have found the infrared emission features to be present in HR 4049, while the 2175 Å bump and the diffuse interstellar bands are absent. This suggests immediately that the infrared emission features and the optical and UV absorption features must arise in different materials (although there are special geometrical arrangements of the circumstellar material that could get around this conclusion).

Most interpretations of the 2175 Å bump attribute it to graphite (Gilra, 1972) or other carbonaceous particles (Greenberg and Chlewicki, 1983; Sakata et al., 1983; Hecht, 1986). The suggestion by Sakata et al., that a carbonaceous material consisting of quenched carbonaceous composite (QCC) is responsible for the bump seemed particularly appealing, because laboratory data and meteoritic spectra (Sakata et al., 1983) show good agreement with the interstellar feature, and because the bump wavelength would be independent of grain size, consistent with observations. We find, however, that QCC's are probably not present in HR 4049 (because they cannot account for the 7.7–8.6 μm features which HR 4049 apparently has), so the lack of 2175 Å absorption in this star does not rule out QCC's as the carriers of this feature in the general interstellar medium.

A recent analysis of the bump by Hecht (1986) provides another interpretation that our data can test. Hecht finds, based on an extensive survey of both theoretical and laboratory data, that if the bump is due to carbon, it must be carbon that is free of contamination due to impurities such as hydrogen. In the circumstellar environment of HR 4049, it is likely that hydrocarbon molecules and grains would form, since the material consists largely of carbon and hydrogen, as indicated by our analysis of the photospheric spectrum. So long as small hydrocarbon grains can retain their hydrogen so close to a hot star, then such grains can be responsible for the far-UV extinction while at the same time not producing any 2175 Å absorption. Indeed, Leene and Cox (1987) show that the particles responsible for the UV extinction bump do not seem to survive strong UV radiation fields. Furthermore, Cox and Leene (1987) showed that the carriers of the UV extinction bump and the mid IR excess are of a different nature.

We note, however, that if hydrocarbon grains can retain their hydrogen so close to a star as hot as HR 4049 it is difficult to envision the circumstances under which these grains would lose their hydrogen under normal interstellar conditions. In order for Hecht's hypothesis to be plausible, there must be a mechanism by which pure carbon grains can form. Our results indicate that this is difficult to do by freeing hydrocarbon grains of their hydrogen.

Perhaps most significant, our results seem to argue against PAH's as the explanation for practically everything, quite the reverse of recent trends. We have shown that PAH's can be responsible for the infrared emission features or the diffuse bands, but probably not both. If we take the majority point of view, that the infrared emission features are due to PAH's, then we appear to have cast severe doubts on ionized PAH's as the carriers of the diffuse bands. On the other hand, other recent work (e.g. Josafatsson and Snow, 1987) indicates that large molecules may be the best candidates for explaining the diffuse bands.

We conclude tentatively that the circumstellar material around HR 4049 contains hydrocarbons in the form of small grains or large molecules. This could explain the UV extinction and the lack of a 2175 Å bump while being consistent with what is known of the composition of the circumstellar material. This picture is viable (in the context of Hecht's analysis at the 2175 Å bump) only if the grains can retain their hydrogen in spite of their exposure to a nearby intense source of ultraviolet photons.

It is interesting to compare the properties of the dust around HR 4049 with those of the dust around R CrB type stars. Hecht et al. (1983) studied the UV extinction of the dust around R CrB and RY Sgr. They show that while the 2175 Å feature is absent, an absorption is seen at 2400–2500 Å, indicating the presence of amorphous or glassy carbon grains with radii between 100 and 500 Å. The IRAS LRS spectra of both stars are essentially featureless (Walker, 1985), no evidence for the presence of PAH's is found. This is in agreement with the chemical composition of the underlying star, for which Cottrell and Lambert (1982) derive a C/H ratio of $4\,10^3$. It is clear that the chemical composition of the underlying star strongly determines the properties of the circumstellar dust grains.

The peculiar star HD 213985 might provide a crucial test for the nature of the carriers of the 2175 Å feature. This star shows a strong IR excess very similar to HR 4049 between 1 and 5 μm (Waelkens et al., 1987), and at the same time a very strong 2175 Å feature of circumstellar origin. Unfortunately, no 3 or 10 μm spectrum is available yet, so that the presence or absence of PAH's is not known. We plan to obtain these observations, as well as diffuse band data, in the near future. The properties of the circumstellar material around HR 4049 and HD 213985 are compared in a forthcoming paper (Buss et al., in preparation).

Acknowledgements. F. Willems is acknowledged for assistance in extracting the IRAS LRS spectra from the database and for valuable suggestions on the interpretation of the LRS spectrum of HR 4049. We thank J. Wollaert for invaluable help in obtaining the one-dimensional co-adds of HR 4049. LBFMW acknowledges financial support from the Netherlands Foundation for Pure Scientific Research ZWO. This project was partly supported by NSF AST8505587. The IRAS data have been processed using the GEISHA analysis system developed by the Laboratory for Space Research and the University of Groningen, Groningen, The Netherlands.

References

Borghesi, A., Bussoletti, E., Colangeli, L.: 1987, *Astrophys. J.* **314**, 422

Cohen, M., Anderson, C.M., Cowley, A., Coyne, G.V., Fawley, W.M., Gull, T.R., Harlan, E.A., Herbig, G.H., Holden, F., Hudson, H.S., Jakoubek, R.O., Johnson, H.M., Merrill, K.M., Schmidt III, F.H., Soifer, B.T., Zuckerman, B.: 1975, *Astrophys. J.* **196**, 179

Cottrell, P.L., Lambert, D.L.: 1982, *Astrophys. J.* **261**, 595

Cox, P., Leene, A.: 1987, *Astron. Astrophys.* **174**, 203

Crawford, M.K., Tielens, A.G.G., Allamendula, L.J.: 1985, *Astrophys. J.* **293**, L45

Dwek, E., Sellgren, K., Soifer, B.T., Werner, M.W.: 1980, *Astrophys. J.* **238**, 140

Federman, S.R., Kumar, C.K. Vanden Bout, P.A.: 1984, *Astrophys. J.* **282**, 485

Gilra, D. 1972, *Ph.D. Dissertation*, Univ. Wisconsin

Greenberg, J.M., Chlewicki, G.: 1983, *Astrophys. J.* **272**, 551

Hecht, J.H.: 1986, *Astrophys. J.* **305**, 817

Herbig, G.H.: 1975. *Astrophys. J.* **196**, 129

IRAS Explanatory Supplement to the Catalogues and Atlases, eds. C.A. Beichman, G. Neugebauer, H.J. Habing, P.E. Clegg, T.J. Chester

IRAS Catalogue of Low Resolution Spectra: 1986, *Astron. Astrophys. Suppl.* **65**, 607

Josafatsson, K., Snow, T.P.: 1987, *Astrophys. J.* **319**, 436

Joshi, U.C., Deshpande, M.R., Son, A.K., Kulshrestha, A.: 1987, *Astron. Astrophys.* **181**, 31

Krelowski, J., Walker, G.A.H.: 1987, *Astrophys. J.* **312**, 860

Kurucz, R.L.: 1979, *Astrophys. J.* **40**, 1

Lambert, D.L., Hinkle, K.H., Luck, R.E.: 1988 *Astrophys. J.* **333**, 917

Lamers, H.J.G.L.M., Waters, L.B.F.M., Germany, C.D., Perez, M.R., Waelkens, C.: 1986, *Astron. Astrophys. Letters* **154**, L20 (Paper I)

Leene, A., Cox, P.: 1987, *Astron. Astrophys. Letters* **174**, L1

Léger, A., Puget, J.L.: 1984, *Astron. Astrophys. Letters* **137**, L5

Mezger, P.G., Mathis, J.S., Panagia, N.: 1982, *Astron. Astrophys.* **105**, 372

Pottasch, S.R.: 1984, in *Planetary Nebulae*, D. Reidel, Dordrecht, p. 206

Puget, J.L., Léger, A., Boulanger, F.: 1985, *Astron. Astrophys. Letters* **142**, L19

Sakata, A., Wada, S., Okutsu, Y., Shintani, H., Nakada, Y.: 1983, *Nature* **301**, 493

Sakata, A., Wada, S., Tanabe, T., Onaka, T.: 1984, *Astrophys. J. Letters* **287**, L51

Sakata, A., Wada, S., Onaka, T., Tokunaga, A.T.: 1987, *Astrophys J. Letters* **320**, L63

Schönberner, D.: 1983, *Astrophys. J.* **227**, 708

Sellgren, K.: 1984, *Astrophys. J.* **277**, 623

Sitko, M.L., Savage, B.D., Meade, M.R.: 1981, *Astrophys. J.* **246**, 161

Sopka, R.J., Hildebrand, R., Jaffe, D.T., Gatley, I., Roellig, T., Werner, M., Jura, M., Zuckerman, B.: 1985, *Astrophys. J.* **294**, 242

Waelkens, C., Waters, L.B.F.M., Cassatella, A., LeBertre, T., Lamers, H.J.G.L.M.: 1987, *Astron. Astrophys. Letters* **181**, L5

Witt, A.N., Schild, R.E.: 1985, *Astrophys. J.* **294**, 225

Wolfire, M.G., Cassinelli, J.P.: 1986, *Astrophys. J.* **310**, 207